Auger-electron emission induced by Ar^+ impact on silicides

S. Valeri, R. Tonini, and G. Ottaviani
Dipartimento di Fisica Università di Modena, via Campi 213/A, I-41100 Modena, Italy
(Received 30 December 1987; revised manuscript received 29 August 1988)

Impact of ions of several kilo-electron-volts (keV) with solids produces inner-shell excitations. The consequent decay results in the emission of Auger electrons whose spectra differ considerably from electrons or x-ray-excited spectra. Si (L_{23}-derived) Auger emission, induced by Ar^+ bombardment in pure Si and silicides of different metals (Cr,Ni,Pt) and stoichiometry (from $NiSi_2$ to Ni_3Si), has been studied by varying both the energy of the primary ions (in the 1–5-keV range) and the takeoff angle (from grazing to normal geometry). We separated the background of inelastic scattered electrons from the Auger electrons, and in a further step the contributions to the spectra coming from deexcitation inside and outside the solid. The portion of the Auger emission which originates from sputtered atoms ("atomic spectrum") was found to depend on the target composition and takeoff angle, being larger in metal-rich silicides and at grazing geometry. The parents of "atomic" Auger electrons were found to be mainly neutral and excited sputtered atoms in Si and Si-rich silicides, while in metal-rich silicides there is a dominant contribution from sputtered ions. These results have been discussed in terms of the inner-shell ionization mechanism and the in-depth distribution of exciting collisions. The "atomic" spectral shape dependencies on ion energy and takeoff angle have been interpreted in terms of the Doppler shift imparted to the Auger-electron velocity by an anisotropic jet of high-energy parent atoms.

I. INTRODUCTION

In the conventional Auger technique an electron beam of energy of a few keV is routinely used to excite inner-shell electrons. The excitation process is a direct Coulomb interaction; little momentum is transferred to the matrix and the excited atom is not displaced from its lattice site. The subsequent Auger decay will generally involve one or two valence-band (VB) electrons, so that the escaping Auger electrons are related to the valence-band density of states and the line shape and energy position of the Auger peak will reflect the target chemical composition. A photon beam in the x-ray energy region is alternatively used as exciting probe. Also in this case the excited atom is not displaced and the Auger process involves the same features as the electron-excited process, apart from differences in the ionization cross section and the absence of autoionization structures.

Ion-beam bombardment can promote inner-shell electrons through crossing of molecular orbitals, as first described for two-particle gas-phase collisions.[1] Atoms can deexcite via the Auger decay channel and the resulting spectra are markedly different from those induced by electrons or photons. The differences are mainly related to the substantial momentum transfer from the projectile to the target atoms because of the similar masses. The target atoms are displaced from their normal lattice site and, because of the short lifetime of inner-shell vacancies (typically 10^{-14} s), the decay can occur in particles in motion in the solid or ejected in the free space, leading to a characteristic atomiclike contribution to the Auger spectra.

In spite of an increasing interest in studies on ion-induced Auger electrons (IAE's), their origin is still controversial and the detailed interpretation of the spectral features is an open problem.[2–6]

In this paper we present the results of an investigation on Auger-electron emission induced by an Ar-ion beam in silicon and silicides of different metal and/or stoichiometry, with the purpose of elucidating the origin of the most relevant structures in the IAE spectra and their behavior versus metal content, projectile energy, and emission angle. The Ni, Pt, and Cr silicides have been chosen because of the detailed knowledge of their electronic properties,[7] electron-induced Auger yield and line shape,[8,9] and sputtering behavior.[10–14]

II. EXPERIMENT

Silicides were prepared by a conventional annealing technique, starting from a metal film of appropriate thickness deposited on polycrystalline Si. The samples were characterized in structure, stoichiometry, and in-depth homogeneity by x-ray diffraction, Rutherford backscattering spectroscopy, and Auger depth profile.

The samples were subsequently introduced in a UHV system (10^{-10} Torr). The surface-cleaning procedure was performed with a differentially pumped Ar^+ gun (5 keV, 5 $\mu A\,cm^{-2}$). This gun was also used as exciting probe for the ion-induced Auger spectra, at ion energies ranging from 1 to 5 keV and ion currents of 2×10^{-3} μA over a spot of 0.2 mm in diameter. The Ar^+-beam direction was at an angle of 55° with the surface normal. Ejected electrons were detected and analyzed using a commercial cylindrical mirror analyzer (CMA), operating in the first derivative mode (0.3% resolution, 1 V peak-to-peak modulation) placed with its axis at 30° with respect to the target surface normal and at about 80° with respect to the incident Ar beam. By an appropriate use of a mechanical shield, we selected the electrons emitted into specific polar angles, namely 12°±2° and 72°±2° with respect to the surface normal. We will refer in the following to these

 ©1988 The American Physical Society

acceptance geometries as "normal" and "grazing" respectively. The CMA coaxial electron gun was also used (E_p=3 keV and I_p=0.1 μA) to obtain conventional electron-induced Auger-electron (EAE) spectra. The ion beam, electron beam, and sample surface were carefully aligned with respect to the CMA, to avoid edge effects in the spectra. The IAE and EAE spectra were subsequently integrated to obtain the N(E) distribution, and the background was subtracted with a spline method.

We focused on the low-energy Si and metal Auger peak in silicides. For comparison, we also measured IAE and EAE spectra in pure Si.

III. RESULTS

In Fig. 1 are shown, in derivative form, the Auger spectra recorded under Ar^+ impact and electron impact on (a) silicon and (b) NiSi at "normal" takeoff angle. The EAE spectra are in good agreement, as it concerns both energy and shape, with previous reported results. In particular, the Si LVV spectrum, which in pure Si presents a single well-defined peak at 92 eV, in Ni silicides splits into four distinct structures. The energy position and relative intensity of these structures are fingerprints of the different compounds in the Si-Ni phase diagram,[10] and the resultant Si LVV line shape has been successfully interpreted in terms of DOS self-convolution.[9] The Si LVV peak shape, and the Si (LVV)–to–Ni (MVV) peak intensity ratio in Fig. 1(b) indicate a slight excess of Si with respect of the correct NiSi stoichiometry, as a consequence of 5-keV sputtering.[10] A comparison with the IAE spectra reveals significant differences. The Si peak of both silicon and silicides presents several structures in the 65–95-eV energy region, the dominant ones being at 88, 95, and 77.5 eV, labeled P_a, P_b, and P_c, respectively, in Fig. 1. Only a small shoulder can be identified at about 92 eV, in correspondence to the main peak in the EAE spectra. In NiSi, the Si-to-Ni peak intensity ratio is strongly reduced in the IAE spectrum with respect to the EAE spectrum. In the IAE spectrum the peak at about 58 eV, due to electrons emitted from Ni atoms, is very weak and does not allow a precise determination of the intensity and energy position; it appears as a broad "dip" at lower kinetic energy (KE) than the corresponding peak in the EAE spectrum.

The IAE spectra for all the silicides we investigated are shown in Fig. 2. A comparison with the corresponding EAE spectra (not reported here) shows that the reduction in intensity and the shift to lower KE of the metal peak are common features for all the compounds. The shifts range from 0.5 to 1.5 eV. This result is qualitatively con-

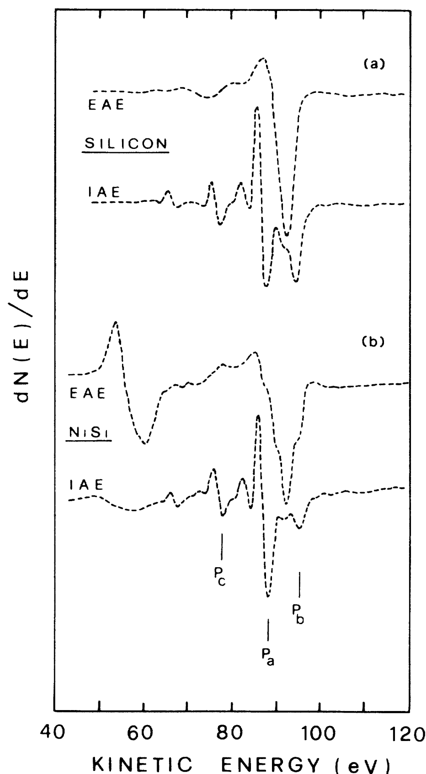

FIG. 1. Electron-excited (EAE) and ion-excited (IAE) Si L_{23}–derived Auger spectra from (a) silicon and (b) NiSi at "normal" takeoff angle.

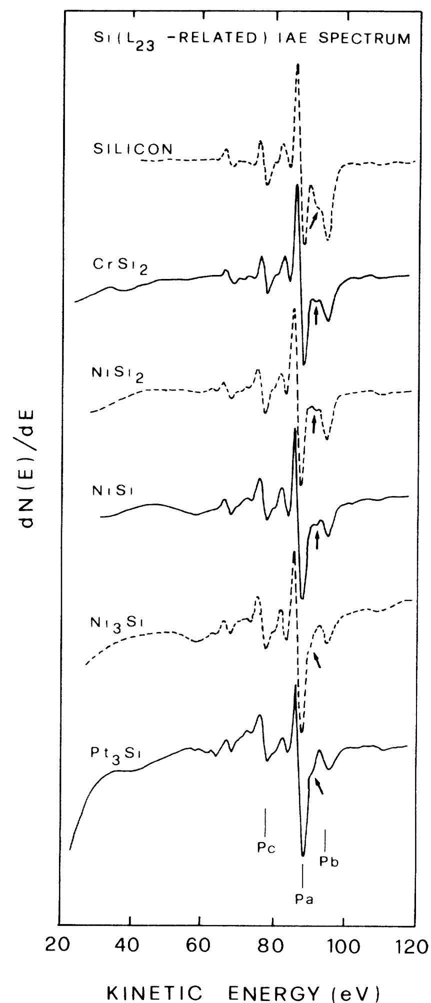

FIG. 2. Si L_{23}–derived IAE spectra from silicon and silicides. The main peaks at 88, 95, and 77.5 eV are labeled P_a, P_b, and P_c, respectively. Arrows indicate the peak associated with the Si LVV transition (see the text).

sistent with the hypothesis that the decay of the excited metal atoms occur out of the solid, but the emitted line of an isolated atom should exhibit a larger shift (3–6 eV). We have at present no explanation for such reduced shifts. We only note that Ar^+-induced Auger spectra in pure metals (Cr,Mn,Fe,Co) show an increase in M_{23}-related Auger peak energy over the corresponding EAE peaks.[15] This suggests that a mechanism is operative, which counteracts the energy lowering related to the "atomic" character of the IAE metal emission.

Regarding the Si peak, it presents a similar shape in all the spectra: the KE of the main structures is independent of whether the Si atoms bonding is covalent (as in pure Si) or metallic (in silicides) and also independent of the partner element and the relative metal-to-Si concentration in the compound. However, there are marked differences in the relative intensities of these structures which can roughly be related to the Si concentration. The 95-eV peak intensity is lower and the 88- and 77.5-eV peak intensity is larger at increasing metal content. We already outlined the presence in Si and NiSi of a small structure located in energy between the 88- and 95-eV peaks. This structure is present in all the silicides, as a well-resolved peak ($CrSi_2$, NiSi, and $NiSi_2$), or as a shoulder in the high-KE side of the 88-eV peak (Pt_3Si and Ni_3Si).

The generally accepted assumption is that the ion-excited Si L_{23}-derived spectra are the superposition of (i) a broad bandlike component, (ii) a series of narrow atomiclike structures, and (iii) a background of inelastically scattered electrons. The separation of these three contributions can be done conveniently in $N(E)$ spectra. We numerically integrated the $dN(E)/dE$ spectra to obtain the $N(E)$ form of both EAE and IAE spectra. Subsequently, the inelastic background subtraction was performed with a spline method. The area of the $N(E)$, background-subtracted Si peak is reported in Fig. 3 versus primary ion energy (E_p) in the range 1–5 keV, at a constant ion density of 6 μA cm^{-2}, for Si, $NiSi_2$, and Pt_3Si; a similar dependence on E_p has been obtained for NiSi, Ni_3Si, and $CrSi_2$, but for clarity we only report in Fig. 3 the area at 5 keV. All the values are normalized to that of pure Si at 5 keV. The Auger yield dependence on E_p is nearly quadratic in the range 1–3 keV as evidenced in Fig. 3 for Si by the comparison with the calculated E^2 dependence of the yield, normalized to the 1-keV value. However, the yield-increasing rate is strongly enhanced at energies higher than 3.5 keV. A strong increase in the Auger yield at projectile energy larger than 4 keV was also reported for Xe^+ ions on gold[16] and Ar^+ ions on silicon[17] and Al.[18]

In Fig. 4 the Si L_{23}-derived IAE peak areas in $M_x Si_{1-x}$ are reported as a function of x, normalized to the value at $x=0$ (e.g., pure silicon). For comparison, we also report in Fig. 4 the corresponding areas of the Si (LVV) EAE peaks for Ni silicides. The x values in this case are set according to the 5-keV ion-induced surface-composition modifications.[10] The EAE Auger yields roughly correlate with the number of Si atoms in the target. With increasing x, the IAE yields decrease much

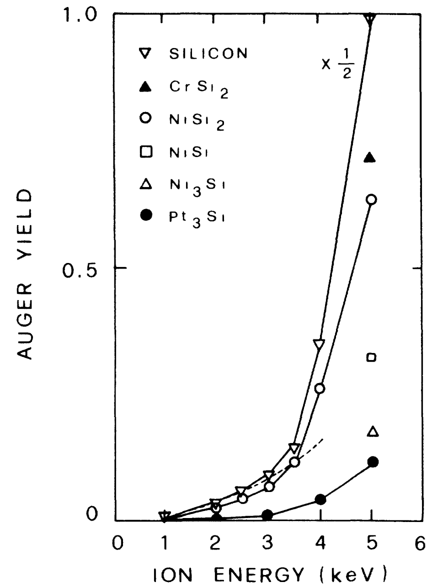

FIG. 3. Dependence of the IAE Auger yield to projectile energy, in silicon, $NiSi_2$, and Pt_3Si. Similar trends have been found for $CrSi_2$, NiSi, and Ni_3Si, but the 5-keV values alone are shown for clarity. All the values are normalized to the 5-keV value in pure silicon. The E_p^2 functional dependence of the yield is also reported, normalized to the 1-keV value in silicon (— — —).

more than the linear decrease of $1-x$. These results are in qualitative agreement with those already reported for the Ni silicides.[19]

Finally, we separated the atomiclike and bulklike contribution by subtracting the EAE spectrum from the IAE spectrum. This procedure is based on two assumptions:

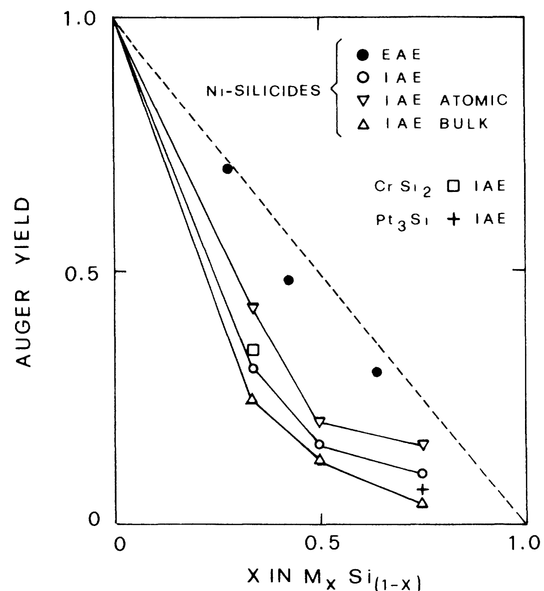

FIG. 4. Si Auger yield dependence on x in $M_x Si_{1-x}$. The yield values are normalized to those in pure silicon. The x values for Si (EAE) yield are set according with the 5-keV ion-induced surface modification (Ref. 10).

(i) the "bulk" contribution in the IAE spectra is satisfactorily represented by the EAE spectra, as claimed by several authors,[2,4,17,18,20–22] and (ii) the IAE spectral intensity in the 92-eV region is mainly due to bulk contribution; consequently, the relative intensities of the EAE and IAE spectra have been chosen in such a way as to have zero intensity in the difference curve in this energy region.[4] This procedure is illustrated in Fig. 5, upper panel, for the $CrSi_2$ case. In the lower panel of Fig. 5 and in Fig. 4 and Table I we show the results of such a data handling. In Fig. 5, lower panel, the atomiclike contributions to the IAE Si spectrum in pure silicon and silicides are reported. They present several structures whose energy positions are insensitive to changes in chemical bonding (from silicon to silicides), in stoichiometry (from Si-rich to metal-rich silicides), and also insensitive to the partner element, supporting the assumption that they are

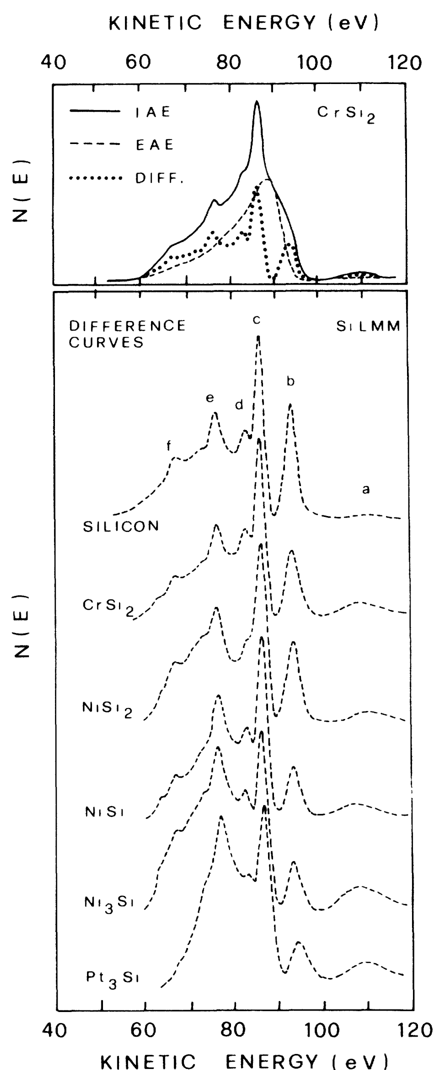

FIG. 5. Upper panel: procedure for the subtraction of the Si $L_{23}VV$ spectrum from the Si IAE L_{23}-derived spectrum, illustrated in the $CrSi_2$ case. Lower panel: the results of such a subtraction (i.e., the Si *LMM* spectra) are shown for silicon and silicides. The peaks are labeled $a-f$ (see the text) and the spectra are normalized to the c peak.

TABLE I. Percent weight of the "atomic" and "bulk" contributions to the 5-keV Si L_{23}-derived IAE spectra in silicon and several silicides.

	Si	$CrSi_2$	$NiSi_2$	NiSi	Ni_3Si	Pt_3Si
Atomic	35	48	53	56	69	66
Bulk	65	52	47	44	31	34

atomic in origin. The main structures are located at about 107.8, 93.7, 86.7, 83, 76.6, and 67 eV and labeled $a-f$ in Fig. 5. Significant differences in the "atomic" spectra of silicides arise from changes in the relative intensity of these structures. In spite of the uncertainties introduced by the background subtraction and difference procedures, and on the low-KE side of the spectra, by the partial overlap of metal peaks in Ni- and Pt-rich silicides, a well-defined trend can be identified in the most relevant spectral features. On passing from pure-Si to Si-rich silicides, we mainly notice the reduced intensity of the b peak with respect to the c one; the a peak, hardly distinguishable in the pure-Si spectrum, became evident. On going to the metal-rich silicides the trend in the a and b peak intensities is confirmed, but the most evident spectral modification is the strong increase in the intensity of the (60–84)-eV region (peaks $d-f$) with respect to the 85–100 -eV region (peaks b and c). The shift of the d structure to lower KE is in our opinion only apparent due to the fact that this structure is just at the separation of two spectral regions whose relative intensities are strongly modified.

The areas of the "atomic" and "bulk" components of the 5-keV Si L_{23}-derived IAE spectra of Ni silicides, normalized to the corresponding ones in pure silicon, are reported in Fig. 4 to have an immediate comparison with the "total" IAE and EAE yields. The "percent weight" of both components of the IAE spectra in pure Si and silicides are shown in Table I. The bulk component, which is the dominant contribution in the pure-Si spectrum, is strongly reduced in silicides with respect to the atomic one. In metal-rich silicides the atomic contribution prevails. A Monte Carlo calculation of the Ar^+-induced Si yield resulted in an atomic emission of 40% of the total,[23] in excellent agreement with our result. This also strongly supports the reliability of the procedure we used to separate the atomic and bulk components of the IAE spectra. Concerning the shape of IAE spectra, with increasing ion energy, we only notice the appearance of the weak peak at 106 eV for energy larger than 3 keV. The spectral shape in the 60–100-eV range is substantially unmodified, indicating that the bulk-to-atomic contribution ratio is independent on the projectile energy. The aluminum IAE atomic-to-bulk yield has been reported to increase with the projectile energy;[23] however, this dependence is strongly reduced at energies larger than 2 keV. In addition, a different criterion for the determination of the atomic-to-bulk yield ratio was used, which also can be responsible for the partial disagreement with our results. When a similar criterion has been used, results in agreement with ours were reported.[21]

All the data presented until now refer to Auger spectra at a takeoff angle of 16° with respect to the surface nor-

mal. The IAE spectra show relevant modifications on passing from this "normal" geometry to "grazing" geometry as shown in Fig. 6 for $NiSi_2$. The main change is the asymmetric broadening of the Auger line shape on the high-KE side. The difference spectrum shown in the same figure clearly indicates that the asymmetric broadening is due to the presence of a sort of "replica" of the sharp atomiclike peaks, rigidly shifted by about 2.3 eV to higher KE. The broadening became more evident with increasing projectile energy (Fig. 7). However, the difference curves in Fig. 7, both referenced to the 2-keV spectrum, show that the larger broadening at 5 keV with respect to 3 keV is mainly due to an increase in the intensity of the shifted contribution, and in minor part to an increase in the shift value (from 2.0 to 2.3 eV). The broadening of the IAE spectra and its dependence on the experimental geometry and projectile energy have been reported on Si,[17,19] Al,[5,24] and silicides.[19] However, the ion energy dependence, is, in general, ascribed to a larger shift of the additional structures.

We outlined that a broadening could be observed in all the structures of the IAE spectrum, in contrast with some reports on a broadening limited to the dominant peaks.[19] We also notice that the 106-eV peak, which only appears at high ion energy, is considerably enhanced in grazing geometry with respect to normal geometry.

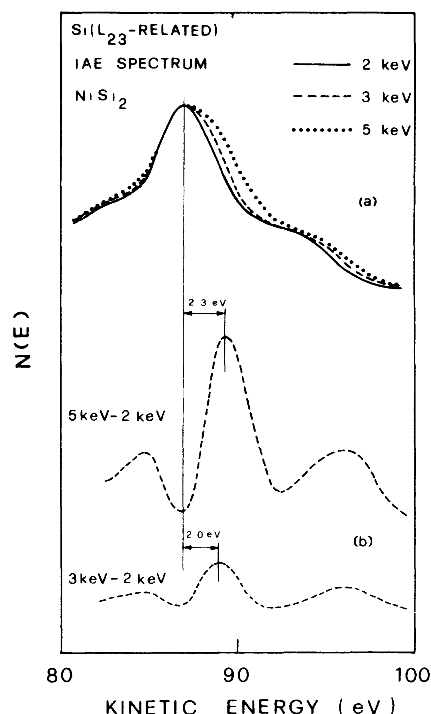

FIG. 7. (a) Normalized Si L_{23}-derived IAE spectra from $NiSi_2$ for bombardment with Ar^+ at different energies. (b) Difference curves relative to the 2-keV spectrum, for the 5- and 3-keV spectra, respectively.

IV. DISCUSSION

In the typical first-derivative form of Si and silicide IAE spectra, the atomiclike and bandlike components were roughly identified in the P_a and P_b peaks located in the 86–87- and 92–95-eV energy regions, respectively. The less intense peaks at approximately 77 and 67 eV were also attributed to atomiclike components. The P_b peak was reported to be located at exactly 92 eV in pure Si and silicides, the same energy as the Si (LVV) EAE spectrum in pure Si.[19] Because of the absence of chemical shifts like those observed in the Si (LVV) spectra of silicides, it was proposed that P_b electrons are emitted from Si atoms beneath the surface but free from the bulk network. Curiously, a very similar explanation was proposed for a completely different result: the 2-eV shift toward higher KE of the P_a peak in the IAE spectrum with respect to the Si (LVV) EAE spectrum in pure Si has been interpreted as due to a markedly different density of states in the collision cascade with respect to the unperturbed case.[17]

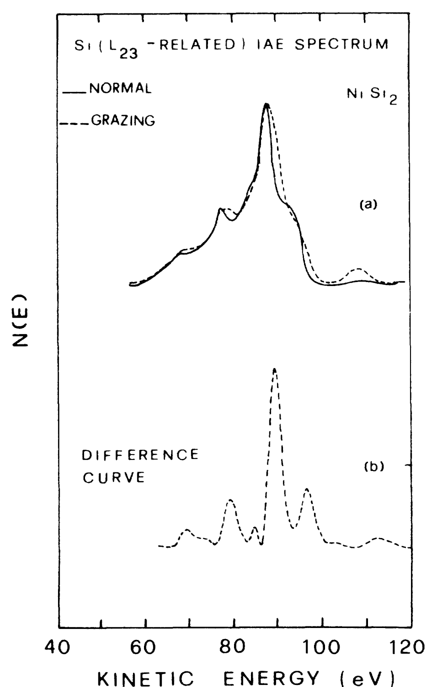

FIG. 6. (a) Normalized Si L_{23}-derived IAE spectra recorded from $NiSi_2$ in "normal" and "grazing" geometry. (b) Difference curve: to obtain this curve, the two spectra in (a) have been normalized at an electron energy of 86.8 eV.

Our results show for the first time the presence of a new peak which is located between P_a and P_b and which energy position changes in various silicides, in agreement with the chemical shifts observed in the silicides Si (LVV) EAE spectra.[7] This peak is clearly due to Auger electrons emitted from Si atoms in the bulk network, it is the "true P_b" peak. This conclusion gives a further support to the assumptions we made for the bulk contribution subtraction from the IAE spectra, namely that the bulk contribution can be represented by the corresponding EAE spectrum and that it is the dominant one at about 90–92 eV.

A. Auger yields

Let us now discuss the results on the Si Auger yield reported in Fig. 4. The usual approach is to correlate the Auger yield to the number of atoms present in the intersection between the excitation and the emission volume. This approach works well for the EAE yields: in the Ni_xSi_{1-x} system the Si (LVV) EAE yields are correctly scaled with x. This approach, however, appears inadequate for the IAE spectra; with increasing x, the yield decrease much more than the linear decrease of $1-x$, as already reported.[19]

A further step is to consider separately the bulk and atomic contributions to the IAE spectra (Fig. 4 and Table I); the first one is expected to be correlated to the Si density, while the second one should be correlated to the Si sputtering yield. However this refinement too is inadequate. The deviation from the linear $1-x$ dependence is even more accentuated for the "bulk" IAE emission. On the other hand, the trend in the available Si sputtering yield in Si and silicides is in complete disagreement with the trend in the "atomic" IAE emission. The most evident example is the comparison between Si and $NiSi_2$. The sputtering yield of Si is enhanced in $NiSi_2$ with respect of pure Si,[14] while the "atomic" IAE yield in the same compound is much less than in pure Si.

The deviations from the expected correlations have been often assumed as an evidence against the generally accepted conclusion, that IAE electrons originate from both Si atoms sputtered out of the specimen surface and Si atoms in bulk network. However, we outline that the expected correlations are based on the assumption of a Si L-shell ionization cross section almost independent of the Si-atom environment. This is the case for electron and photon probes, but it is questionable for ion probes, due to the different ionization mechanism. The electronic excitations are assumed to occur via close coupling among molecular orbitals (MO's) transiently formed during the collision, the Si L-shell excitations being described essentially in terms of $4f\sigma$-electron promotion, according to the original Fano-Lichten[1] electron-promotion model recently modified by Schneider *et al.*[25] The MO electron-promotion process only occurs if the minimum internuclear distance in the collision falls below a "critical" distance R_c. R_c ranges between 0.3 and 0.5 Å for Ar on light elements, and, in particular, electron promotion of the Si $2p$ electron in Ar-induced collisions was reported to occur at $R_c = 0.37$ Å.[21] A possible explanation is that the projectile or a recoiled target atom's probability of approaching a Si atom closer than R_c is reduced in silicides, where Si atoms are surrounded by "larger" metal atoms, with respect to pure Si. A further reduction is expected when the number of metal atoms adjacent to Si atoms increases (e.g., on going from Si-rich to metal-rich silicides), in agreement with our results on the IAE Auger yield. We can also suggest a possible contribution from the chemical bonding, because the Auger yield is extremely sensitive to the actual number of electrons occupying the Si M-shell prior to decay. This number is, in turn, determined by the charge state of the Si atom before the collision and by the L-to-M shell excitation during the collision (see next paragraph).

The insensitivity of Si IAE line shape to E_p suggests that both atomic and bulk Auger yields depend in a very similar way on projectile energy. Therefore the dependence of Auger yield on E_p should be essentially related to the excitation process. The ionization can occur via symmetric or asymmetric collisions, the latter in the direct projectile-target collision and the former in the subsequent cascade process within the solid. It was shown by computer simulation that the probability of creating $2p$ core holes in Si atoms by the electron-promotion process is a quadratic function of the projectile energy in symmetric collision.[23] Figure 3 shows an Ar-ion energy dependence of the Auger yield of E^2 in the 1–3-keV range in both Si and silicides; we can conclude that in the low-projectile-energy range the dominant ionization process is the symmetric Si-Si collision within the cascade. We believe that the enhanced efficiency observed above 3 keV should be attributed to a marked contribution of the asymmetric Ar-Si collision to Si $2p$ excitation, as already suggested for Ar impact above 4 keV on pure Si (Ref. 17) and Al.[18]

These considerations refer to the total IAE yield, no matter whether the decay occurs outside or inside the solid; however, it is also interesting to note the trend in the atomic-to-bulk yield ratio (Table I). This ratio increases by a factor 2 in Si-rich silicides, and of a factor 4 in metal-rich silicides, with respect to pure Si. The relative probability for the atom with a $2p$ core hole to decay inside or outside the solid depends on the core-hole lifetime, and on the time that the atom spends in the solid before escaping. This time is related to the momentum transferred to the atom in the collision, and to the depth at which the collision occurs. The Si $2p$ core-hole lifetime is assumed not to vary appreciably in silicides, as indicated by the near constant width of the Si $2p$ peak in photoemission spectra from Si and silicides.[26,27] We performed numerical simulations based on a Monte Carlo method[28] to obtain the amount and the in-depth distribution of the energy transferred to the Si recoils in a 5-keV Ar^+ collision with Si or silicides. Simulations at 2 keV Ar^+ energy have been also performed in Si and $CrSi_2$ case. The results are reported in Table II and enable us

TABLE II. Total energy (eV/Å) imparted by 5-keV Ar^+ projectile to target Si atoms, normalized to Si atomic density in the target. Also shown is the distance (Å) from the surface of the maximum of the in-depth distribution of the total energy transferred to target Si atoms. In parentheses, the corresponding values calculated for 2-keV Ar^+ on Si and $CrSi_2$ are reported.

	Total energy (eV/Å)	Distance (Å)
Si	8 (5)	40 (25)
$CrSi_2$	9 (6)	25 (13)
$NiSi_2$	8	28
NiSi	8	23
Ni_3Si	10	18
Pt_3Si	10	16

to conclude that the increased contribution of the atomic yield to the total IAE yield at increasing metal content is due to a larger energy transfer to Si atoms in a shallower region in metal-rich silicides with respect to Si-rich silicides and pure Si. The atomic-to-bulk yield ratio is for a given target almost independent of E_p. A comparison between the 2- and 5-keV results of Table II provides a possible, at least qualitative, explanation. At higher projectile energy, the collision occurs deeper in the solid; however, a larger energy is transferred to the Si atom; the latter effect counteracts the former one. This contributes to the substantially unaltered probability of the inner-shell excited Si atom being sputtered from the solid before decay.

B. Auger line shapes

As far as the atomiclike features are concerned, we adopt the interpretation of Ref. 2: the atomic peaks are associated with excited neutral atoms or ions decaying in free space. Referring to Fig. 5, structures labeled *b* and *c* are assigned to transition in Si neutral atoms with a $2p$ vacancy (Si^0) (from the $2p^53s^23p^3$ configuration to $2p^63s^23p$ and $2p^63s3p^2$, respectively), while structures labeled *e* and *f* are assigned to transitions in Si ions with a $2p$ vacancy (Si^+) (from the $2p^53s^23p^2$ configuration to $2p^63s3p$ and $2p^63s^2$, respectively). The peak *a* at 106 eV is assigned to transitions in Si ions with a double $2p$ vacancy (Si^{2+}) (from $2p^43s^23p^3$ to $2p^53s3p^2$). Si double ionization only originates in asymmetric collisions.[29,30] The occurrence of this peak at an ion energy larger than 3 keV confirms the conclusions of the preceding paragraph as it concerns the relative contribution of symmetric and asymmetric collisions to the Auger yield.[29,30] We cannot unambiguously assign the small structure labeled *d*, which on the basis of Ref. 2 presents probably a mixed Si^0+Si^+ character.

We first focus on the trend in the relative intensity of the Si^0, Si^+, and Si^{2+} contributions versus Si content. By increasing the metal content, the intensity of the 65–85-eV spectral region, mainly Si^+ related, strongly increases with respect to the 85–100-eV region, which is Si^0 related; the 106-eV peak (Si^{2+}) also increases. Two mechanisms have been proposed for the neutral-excited emission[2]: (1) it is possible that the $2p$ electron be promoted to the $3p$ level by the curve-crossing mechanism, in a sort of "autoionization" process, and (2) an ion with a single $2p$ vacancy, recoiling from the target, could possibly extract an electron from the valence band into the $3p$ level by a charge-transfer process.

The neutralization efficiency is determined by the number of available free electrons in the region crossed by the ions, for low-energy ions, and by the residence time in this region.[31] The free-electron density in metalliclike systems (silicides) is much higher than on the surface of the semiconductor (Si), and increases with the metallic character of the bonding, i.e., with metal content in silicides. From the results of Table II we deduce that at increasing metal content the recoils should have a higher velocity and a reduced path in the solid before escape, but we believe that this only partially compensates for the increase in the neutralization efficiency. Therefore on the basis of mechanism (2) we expect a larger Si^0-related contribution in the atomic spectra of metal-rich silicides with respect to Si-rich silicides and pure Si, just the opposite of our findings. The efficiency of the mechanism (1) is related to the availability of empty states just above the Fermi level. The Auger process being an atomic, well-localized process, the states we are dealing with are the Si *sp* empty states. On passing from pure Si to silicides, and from Si-rich to metal-rich silicides, the density of these states above Fermi level is reduced,[7,32,33] in agreement with the trend in the Si^0 contribution (Fig. 5). We conclude that mechanism (1) is the dominant one in the neutral-excited emission.

A second aspect is the angular dependence of the Auger line shape. First, we note that the additional shifted contribution in the "grazing" spectrum (difference curve in Fig. 6) is not exactly a replica of the "normal" spectrum. The neutral-to-ion ratio contribution increases on going at grazing emission, even more than appears in Fig. 6, if we consider that the bulk contribution to the spectrum is reduced according with the $(\cos\theta)^{-1}$ law. This can be attributed to the reduced lifetime of the neutral excited states with respect to the ion states, due to the presence of the additional electron (in the *M* shell) which enhances the number of decay channels. The lifetime reduction was estimated at a factor 2 in Si.[23] The most likely cause of broadening is the distribution in Doppler shifts due to the distribution of velocity components of the decaying atoms in the direction of observation.[5,17,19,24] Most of the sputter-induced Si ejection is isotropic and of low energy, but an additional flux of high-energy Si is anisotropically ejected from the surface in a direction close to the projection of the ion beam on the target surface.[5]

Due to our experimental geometry, in the "grazing" configuration the analyzer is partially "looking into" the incident-ion beam and the high-energy Si flux has a significant component of its velocity toward the analyzer. The electrons emitted parallel to the flux acquire a positive Doppler shift $\Delta E = 0.07\sqrt{E(\text{eV})}\cos\theta$,[5] where θ is the angle between the direction of motion of the electron and of the parent atom, and E is the KE of the parent atom.

From the maximum electron-energy shift (2.3 eV), and taking into account our experimental geometry, we estimate the maximum KE of the Si jet to be $\simeq 1400$ eV. This value is far greater than the kinetic energy of the average sputtered atom (typically few eV), however high KE for sputtered atoms with inner-shell vacancies has been reported.[23] Such a high value also suggests that the anisotropic emission is due to asymmetric Ar-Si collision in the surface layer, because symmetric collisions in the cascade should share the projectile energy among the collision partners and lead to lower ejection energies. This origin of the parent atoms responsible for the Doppler shift is also consistent with their asymmetric distribution, because the emission resulting from the random collisions within the cascade is expected to be isotropic and is supported by the enhancement of the 106-eV peak, strictly related to asymmetric collision, in grazing geometry. A

1.6-eV Doppler shift of the L_{23}-derived IAE peak has been already observed in Al.[5] The larger value we observed for Si is in accord with the calculated ejection energy of excited atoms, higher in Si than in Al.[23]

The Si *LMM* spectral shape in the grazing configuration is ion-energy dependent: the asymmetric broadening in Si *LMM* spectral shape is larger at increasing ion energy. This is in agreement with previous results on Si and Al,[24,5,17] in general interpreted as consistent with the Doppler effect: the KE of the ejected atoms is expected to increase for higher E_p; thus the Doppler shift of the Auger electrons is larger. However, we observed that the ion energy mainly determines the number of electrons which experience the Doppler shift, and only marginally the amount of the shift (Fig. 7). This can be qualitatively understood on the basis of the data of Table II. By increasing E_p the collisions extend deeper into the solid, and a larger number of Si atoms can be emitted. However, the larger energy imparted to a Si atom is partially counterbalanced by energy loss which occurs during the travel of the sputtered atom through the solid.

V. CONCLUSIONS

Our study has led to the following conclusions.

(i) All the prominent peaks in the usual $dN(E)/dE$ form of the Si L_{23}-derived IAE spectra of Si and silicides originate in sputtered, 2*p*-excited Si atoms and ions. A small, often poorly resolved peak has been identified, which can be assigned to emission from excited Si atoms decaying in the bulk.

(ii) The IAE yield dependence on projectile energy and target composition is essentially related to the excitation process.

(iii) The atomic-to-bulk IAE yield ratio strongly depends on target composition, being larger in metal-rich silicides than in Si-rich silicides and pure Si. This has been attributed to the fact that in Si and Si-rich silicides the ionization occurs deeper into the solid, and a larger number of excited atoms removed from their lattice sites decay before they escape in the vacuum.

(iv) The $2p \rightarrow 3p$ electron promotion (autoionization) during the collision is the predominant mechanism in the neutral-excited emission. The relative weight of the IAE contributions which originate from neutral excited atoms or ions, respectively, is correlated with the Si *sp* empty-state density just above the Fermi level.

(v) In grazing emission the larger contribution to the IAE atomic spectrum from sputtered neutral-excited atoms with respect to normal emission support the idea of a reduced lifetime of the neutral-excited state with respect to the ion state. The projectile-energy dependence of the "Doppler shift," observed in grazing geometry, is mainly due to an increase in the number of "fast" parent atoms, and in minor part to an increase of their KE, again in agreement with the amount and the in-depth distribution and of the energy transfer to Si atoms.

ACKNOWLEDGMENTS

The authors are indebted to E. Angeli for useful technical collaboration. This work was supported by Centro di Calcolo, Università di Modena and by Gruppo Nazionale Struttura della Materia–Consiglio Nazionale delle Ricerche, and Ministero della Pubblica Istruzione.

[1]U. Fano and W. Lichten, Phys. Rev. Lett. **14**, 627 (1965); W. Lichten, Phys. Rev. **164**, 131 (1967); M. Barat and W. Lichten, *ibid.* A **6**, 211 (1972).

[2]E. W. Thomas, Vacuum **34**, 1031 (1984).

[3]R. Whaley and E. W. Thomas, J. Appl. Phys. **56**, 1505 (1984).

[4]M. Negre, J. Mischler, and N. Benazeth, Surf. Sci. **157**, 436 (1985).

[5]S. V. Pepper and P. R. Aron, Surf. Sci. **169**, 14 (1986).

[6]L. De Ferraris, O. Grizzi, G. E. Zampieri, E V. Alonso, and R. A. Baragiola, Surf. Sci. **167**, L175 (1986).

[7]C. Calandra, O. Bisi, and G. Ottaviani, Surf. Sci. Rep. **4**, 271 (1984).

[8]J. A. Roth and C. R. Crowell, J. Vac. Sci. Technol. **15**, 1317 (1978).

[9]U. del Pennino, P. Sassaroli, S. Valeri, C. M. Bertoni, O. Bisi, and C. Calandra, J. Phys. C **16**, 6309 (1983).

[10]S. Valeri, U. del Pennino, P. Sassaroli, and G. Ottaviani, Phys. Rev. B **28**, 4277 (1983).

[11]S. Valeri and G. Ottaviani, J. Vac. Sci. Technol. A **5**, 1358 (1987).

[12]Th. Wirth, V. Atzrodt, and H. Lange, Phys. Status Solidi A **82**, 459 (1984).

[13]S. Valeri, U. del Pennino, and P. Lomellini, Thin Solid Films **130**, 315 (1985).

[14]S. C. Kim, S. Yamaguchi, Y. Kataoka, M. Iwami, A. Hiraki, M. Satou, and F. Fujimoto, Jpn. J. Appl. Phys. **21**, 39 (1982).

[15]K. O. Legg, W. A. Meta, and E. W. Thomas, J. Appl. Phys. **51**, 4437 (1980).

[16]E. V. Alonso, M. A. Alurralde, and R. A. Baragiola, Surf. Sci. **166**, L155 (1986).

[17]K. Wittmaack, Surf. Sci. **85**, 69 (1979).

[18]O. Grizzi and R. A. Baragiola, Phys. Rev. A **35**, 135 (1987).

[19]M.Iwami, S. C. Kim, Y. Kataoka, T. Imura, A. Hiraki, and F. Fujimoto, Jpn. J. Appl. Phys. **19**, 1627 (1980).

[20]J. Mischler and N. Benazeth, Scanning Electron Microsc. **II**, 351 (1986).

[21]C. Benazeth, N. Benazeth, and M. Hou, Surf. Sci. **151**, L137 (1985).

[22]J. Mischler, N. Benazeth, M. Negre, and C. Benazeth, Surf. Sci. **136**, 532 (1984).

[23]T. D. Andreadis, J. Fine, and J. A. D. Mattew, Nucl. Instrum. Methods **209/210**, 495 (1983).

[24]R. A. Baragiola, E. V. Alonso, and H. J. L. Raiti, Phys. Rev. A **25**, 1969 (1982).

[25]D. Schneider, G. Nolte, U. Wille, and N. Stolterfoht, Phys. Rev. A **28**, 161 (1983).

[26]A. Franciosi, J. H. Weaver, and F. A. Schmidt, Phys. Rev. B **26**, 546 (1982); P. J. Grunthaner, F. J. Grunthaner, and J. W.

Mayer, J. Vac. Sci. Technol. **17**, 924 (1980).

[27]S. Valeri, U. del Pennino, P. Lomellini, and P. Sassaroli, Surf. Sci. **145**, 371 (1984).

[28]J. F. Ziegler, J. P. Biersack, and U. Littmark, *The Stopping and Range of Ions in Solids* (Pergamon, New York, 1985).

[29]P. Viaris de Lesegno and J. F. Hennequin, Surf. Sci. **103**, 257 (1981).

[30]J. F. Hennequin, R. L. Inglebert, and P. Viaris de Lesegno, Surf. Sci. **140**, 197 (1984).

[31]*Inelastic Ion Surface Collisions,* edited by N. H. Tolk, J. C. Tully, W. Heiland, and C. W. White (Academic, New York, 1977).

[32]J. H. Weaver, V. L. Moruzzi, and F. A. Schmidt, Phys. Rev. B **23**, 2916 (1980).

[33]A. Franciosi, J. H. Weaver, D. G. O'Neil, F. A. Schmidt, O. Bisi, and C. Calandra, Phys. Rev. B **28**, 7000 (1983).